THE EUROPEAN
PHYSICAL JOURNAL A

Regular Article – Experimental Physics

Investigation of the threshold anomaly in the near-barrier elastic scattering of ^{7}Li on ^{116}Sn

N.N. Deshmukh[1,2,a], S. Mukherjee[1], B.K. Nayak[3], D.C. Biswas[3], S. Santra[3], E.T. Mirgule[3], S. Appannababu[1], D. Patel[1], A. Saxena[3], R.K. Choudhury[3], J. Lubian[4], and P.R.S. Gomes[4]

[1] Department of Physics, Faculty of Science, The M.S. University of Baroda, Vadodara, 390 002, India
[2] Physics Department, Degree (First Shift), Parul Institute of Engineering & Technology, Limda, Waghodia, Vadodara, 391 760, India
[3] Nuclear Physics Division, BARC Mumbai, 400085, India
[4] Instituto de Física, Universidade Federal Fluminense, Niteroi, R.J., 24210-340, Brazil

Abstract. Elastic-scattering angular distributions of ^{7}Li on ^{116}Sn have been measured at different bombarding energies between 18 to 35 MeV. The effects of the weakly bound projectile breakup channel on the bombarding energy dependence of the interaction potential have been investigated. In this work we present the experimental results, along with the theoretical analysis using Woods-Saxon potential to investigate the energy dependence of the interacting polarizing potentials. Total reaction cross-sections are also presented and discussed.

1 Introduction

During the last few years, the scattering of weakly bound nuclei colliding at energies near and below the Coulomb barrier has been a subject of great interest. The energy dependence of the optical potential (OP) of the elastic scattering of tightly bound nuclei, at near-barrier energies, shows a rapid variation of both the real and imaginary parts of the potential. This energy dependence is produced by polarization potentials originated from the coupling between the elastic scattering and different reaction channels, such as inelastic excitations, transfer of nucleons, breakup etc. Dynamic polarization potential, or simply polarization potential, is such that when it is added to the bare energy-independent potential, it produces the same elastic-scattering cross-section as the one obtained with coupled channel calculations. The net effect on the energy dependence of the optical potential depends on the importance and strength of the different specific polarization potentials. For systems containing only tightly bound nuclei, couplings to bound excited states or transfer channels produce an attractive polarization potential. This additional attraction of the real potential decreases the Coulomb barrier, consequently enhancing the fusion cross-section, when compared with no-coupling calculations. This phenomenon has been named threshold anomaly (TA) [1–3]. The energy dependences of the real

and imaginary potentials are related to each other and are consistent with a dispersion relation [1–3]. The basic characterization of the TA is the observation of a localized peak in the real part of the potential accompanying a sharp decrease of the imaginary part as the bombarding energy decreases towards the Coulomb barrier. The behaviour of the imaginary part of the potential is related with the closing of reaction channels when the energy approaches or is smaller than the Coulomb barrier.

When at least one of the colliding nuclei is weakly bound, the situation changes because the breakup channel may become important and this channel has excitation function that does not drop sharply at energies below the Coulomb barrier. Furthermore, the breakup channel feeds states in the continuum, that only under some spatial restrictions goes back to fusion. So, the net polarization potential in the scattering of weakly bound nuclei has two components: an attractive one, due to the couplings of the elastic channel with inelastic excitations and other direct reactions and a repulsive one, due to the breakup. If the attractive potential predominates, the behaviour of the net polarization potential is such that TA is still observed. However, if the repulsive polarization potential predominates, one says that the system presents the Breakup Threshold Anomaly (BTA) [4,5]. In the original paper describing this phenomenon [5], it was mentioned that the BTA is characterized by the increase of the imaginary potential as the energy decreases towards the barrier. Nevertheless, BTA might also be interpreted as the absence of

a e-mail: nikitdesh@yahoo.com

the TA due to the breakup channel [6], and consequently energy-independent real and imaginary potentials.

The investigation of the presence of TA, BTA or energy-independent optical potentials through the analysis of elastic-scattering angular distributions is a very difficult task, since the desired manifestation of the optical potential behaviour can only be assessed near and below the barrier energies, where the elastic scattering is predominantly of Rutherford type, and small deviations from it may only be obtained from very precise measurements. Even so, the low sensibility of the nuclear interacting potential at such low energies with the corresponding elastic-scattering data leads to large error bars in the determination of such potentials. Satchler [2] has already addressed this difficulty and, recently, complementary measurements on that direction were adopted by Zerva $et\ al.$ [7,8] by the backscattering technique.

In a recent work we have investigated the elastic scattering of the ^{6}Li $+$ ^{116,112}Sn systems [9]. A clear BTA behaviour was observed, with the imaginary potential increasing when the bombarding energy decreases towards the barrier. This behaviour was found to be consistent with the systematics obtained from the elastic scattering of ^{6}Li on different targets, from ^{27}Al to ^{209}Bi (^{27}Al, ^{58}Ni, ^{64}Ni, ^{64}Zn, ^{90}Zr, ^{144}Sm, ^{208}Pb and ^{209}Bi) [4,5,10–17]. For the scattering of ^{7}Li the situation is not so clear. The ^{7}Li nucleus has breakup $(\alpha + t)$ threshold energy of 2.47 MeV and one bound excited state at 0.48 MeV. As pointed out by Lubian $et\ al.$ [18], since ^{7}Li has one bound excited state and the stripping of one neutron may have large positive Q values for several target nuclei, the attractive component of the dynamic polarization potential in the scattering of this projectile may be comparable or even predominates over the repulsive dynamic polarization potential due to the breakup. The net result may vary qualitatively for different targets, since the strengths and the interference between the different polarization potentials may be different. Actually, a systematic behaviour for the energy dependence of the optical potential in the scattering of ^{7}Li has not been reached so far, since the few systems investigated in the literature (^{27}Al, ^{28}Si, ^{59}Co, ^{138}Ba, ^{144}Sm, ^{208}Pb) [4,15,16,19–24] show different behaviours. Particularly for medium-heavy targets, there is only one work on the ^{144}Sm target [15], where nearly energy-independent real and imaginary potentials were observed. For the ^{138}Ba target, different analyses lead to different conclusions [4, 23,24].

In order to contribute to obtain a more clear picture of a possible systematic behaviour for the optical potential in the near-barrier scattering of ^{7}Li, we performed measurements of elastic scattering for the ^{7}Li $+$ ^{116}Sn system, also filling the gap between $A = 59$ and 144 for the target mass. The energy range of the measurements is from 20% below the Coulomb barrier to 70% above the barrier. The total reaction cross-sections have also been extracted by the optical model fitting of the experimental data and they are compared with those from the ^{6}Li $+$ ^{116}Sn system.

In sect. 2, we give experimental details of this work. In sect. 3, an optical model analysis of the measured elastic-scattering angular distributions is presented in order to study the energy dependence of the interaction potential at near-barrier energies. The derived reaction cross-sections are compared with the ones for the ^{6}Li $+$ ^{116}Sn system in sect. 4. Finally, we derive some conclusions in sect. 5.

2 Experimental details

The experiment was performed at the Bhabha Atomic Research Centre - Tata Institute of Fundamental Research (BARC-TIFR) pelletron facility, Mumbai, India. The beam of ^{7}Li was delivered by the 14UD Pelletron accelerator. The elastic-scattering angular distributions were measured for ^{7}Li beam at ten different bombarding energies starting from below the Coulomb barrier, namely, 18, 19, 20, 21, 22, 23, 24, 26, 30 and 35 MeV. The nominal Coulomb barrier for this system is around 23 MeV in the laboratory frame. The beam was bombarded on a 430 μg/cm^2 self-supported enriched ^{116}Sn ($\geq$ 98%) target and the elastically scattered ^{7}Li ions were detected by four solid-state silicon surface barrier $\Delta E + E$ telescopic arrangements. The telescopes used were of different thicknesses (T_1 with $\Delta E = 40\,\mu$m and $E = 1500$ mm thick, T_2 with $\Delta E = 15\,\mu$m and $E = 1500$ mm thick, T_3 with $\Delta E = 25\,\mu$m and $E = 1000$ mm thick, and T_4 with $\Delta E = 25\,\mu$m and $E = 1000$ mm thick). One monitor of thickness $600\,\mu$m was used for the absolute normalization. The telescopes were placed on a rotating arm inside a 1 m diameter scattering chamber at an angular separation of 10° between consecutive telescopes. The monitor was fixed at the forward angle 30°. Beam currents were ranging between 7 and 40 nA. The angular distributions were measured in steps of 2.5° to 5° at angles from 20° to 173° at lower energies and from 20° to 105° for higher energies. The uncertainty in the detector angular position is 0.1 degrees. The statistical error in this system was found out to be less than 5% in the case of forward angles and a maximum of 30% in the case of backward angles. From the known abundances of the Sn target the contribution from the contaminants of the target was estimated to be about 1%. The detectors solid angles uncertainty is 2%. When one adds the uncertainties in the angular position, in the beam angle and in the beam spot position one estimates the overall systematic uncertainty in the normalization as ±6.0%. So, the overall errors in the cross-sections are from 8.0% and 31%.

3 Optical-model analysis of elastic-scattering angular distribution

The phenomenological Woods-Saxon potential has been used to fit the elastic-scattering angular distribution data by using the ECIS code [25].

The optical-model potential used to extract the elastic-scattering differential cross-sections is given by the following equation:

$$U(r) = V_{\mathrm{coul}}(r) - V_r f(r, R_r, a_r) - i W_i f(r, R_i, a_i), \quad (1)$$

where V_{coul} is the Coulomb potential of a uniformly charged sphere of radius $R_c = 1.25(A_p^{1/3} + A_t^{1/3})$ fm, A_p and A_t being the mass numbers of the projectile and target, respectively; f represents the Woods-Saxon form function which is given by $f(r, R, a) = [1 + \exp(r - R/a)]^{-1}$, where R is the radius and a is the diffuseness; r_i is the reduced radius, defined as $R_i = r_i(A_p^{1/3} + A_t^{1/3})$. Accordingly, the third term in eq. (1) represents the volume imaginary potential of the optical potential U and W_i symbolizes its depth. The second term is the real part of the potential U, where V_r symbolizes its depth.

As we did not divide the imaginary part of the optical potential into two parts (volume + surface), the whole absorption due to the inelastic scattering, transfer channels, breakup and fusion processes is taken care by the volume imaginary potential of the optical potential U. This phenomenological framework contains six parameters, *i.e.*, V_r and W_i, namely, the two depths, R_r and R_i, namely, the two radii, a_r and a_i, namely, the two diffusenesses. These quantities may be free parameters to fit the experimental differential cross-sections. However, by varying such a large number of parameters one may obtain unrealistic physically values. Therefore, it is usual to keep some fixed parameters in the fit procedure.

The fitting procedure of the data was performed by changing only the real and imaginary depths of the potential and by keeping the real and imaginary reduced radii as 1.06 and 0.53 fm, respectively. After the first fit was obtained, we once again kept the radii fixed and varied the diffusivity of the potentials from 0.49 to 0.57 fm in steps of 0.02 fm and the depths of the real and imaginary potentials were fitted. For the lowest three energies, the diffuseness of the potentials was reduced to 0.45 fm in order to obtain attractive real nuclear potential and absorption of flux. As it usually happens in this kind of analysis, although very good fits were obtained, several families of optical-potential parameters that describe the angular distributions fitted equally well the data. These ambiguities are removed by evaluating the potential at the sensitivity radii R_{Sr} and R_{Si} [2], corresponding to the real and imaginary potential, defined as the value of the radii for which different potentials with similar good fits have the same value. The derived mean sensitivity radii were 10.42 and 8.95 fm for real and imaginary potential, respectively. Figures 1(a) and (b) show, for the energy of 23 MeV, families of potentials that give similar fits, and the crossing points corresponding to the sensitivity radii for the real and imaginary parts, respectively. Finally the energy dependence of the interacting potentials were determined with an average sensitive radius $R_S = 9.685$ fm, *i.e.*, the average between R_{Sr} and R_{Si}, along with the mean diffuseness $a = 0.53$ fm for highest energies and $a = 0.45$ fm for lowest energies. Figure 2 shows the experimental elastic scattering angular distributions and the best fit obtained, with the parameters shown in table 1. The corresponding values of the energy dependence of the interacting potentials are shown in fig. 3. The error bars in fig. 3 represent the range of deviation of the potential corresponding to a χ^2 variation of one unit. For energies where χ^2 is much
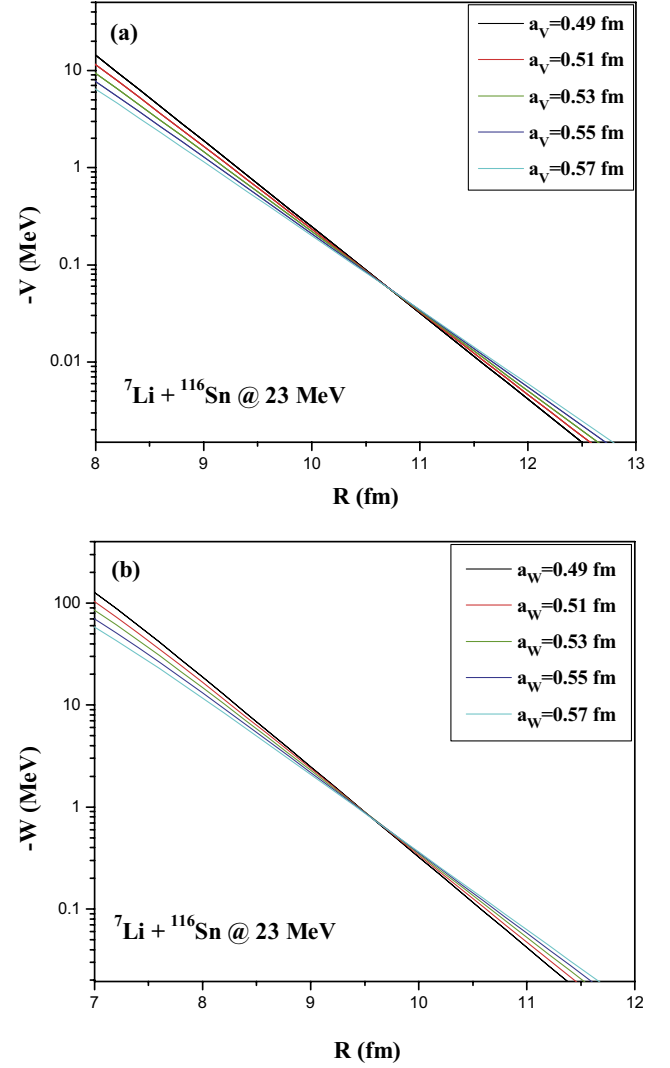

Fig. 1. (Color online) Different families of potential parameters that produce similar fits of the data, at 23 MeV. The real and imaginary sensitivity radii are the values where they intersect each other, respectively, in (a) and (b).

larger than the unity (21 MeV, 24 MeV and 35 MeV), this criterion leads to unrealistic small error bars, as it can be observed in fig. 3.

From fig. 3 it is observed that real and imaginary parts of the interacting potentials are quite energy independent at energies higher than the Coulomb energy. However, it can be observed that at energies below the Coulomb barrier the imaginary part of the OP does not drop to zero, but rather there is a small increment indicating the absence of the TA. One can also see an almost constant trend of the real potential at lower energies, instead of the characteristic bell shape that corresponds to the TA. This behaviour is very similar to the one observed for the $^7\mathrm{Li} + {}^{144}\mathrm{Sm}$ system [15]. For the much lighter $^7\mathrm{Li} + {}^{27}\mathrm{Al}$ system [21], both the real and imaginary potentials show almost energy-independent behaviours. For any of those systems, there is no evidence of the presence of the TA. The BTA behaviour, with a sharp increase of
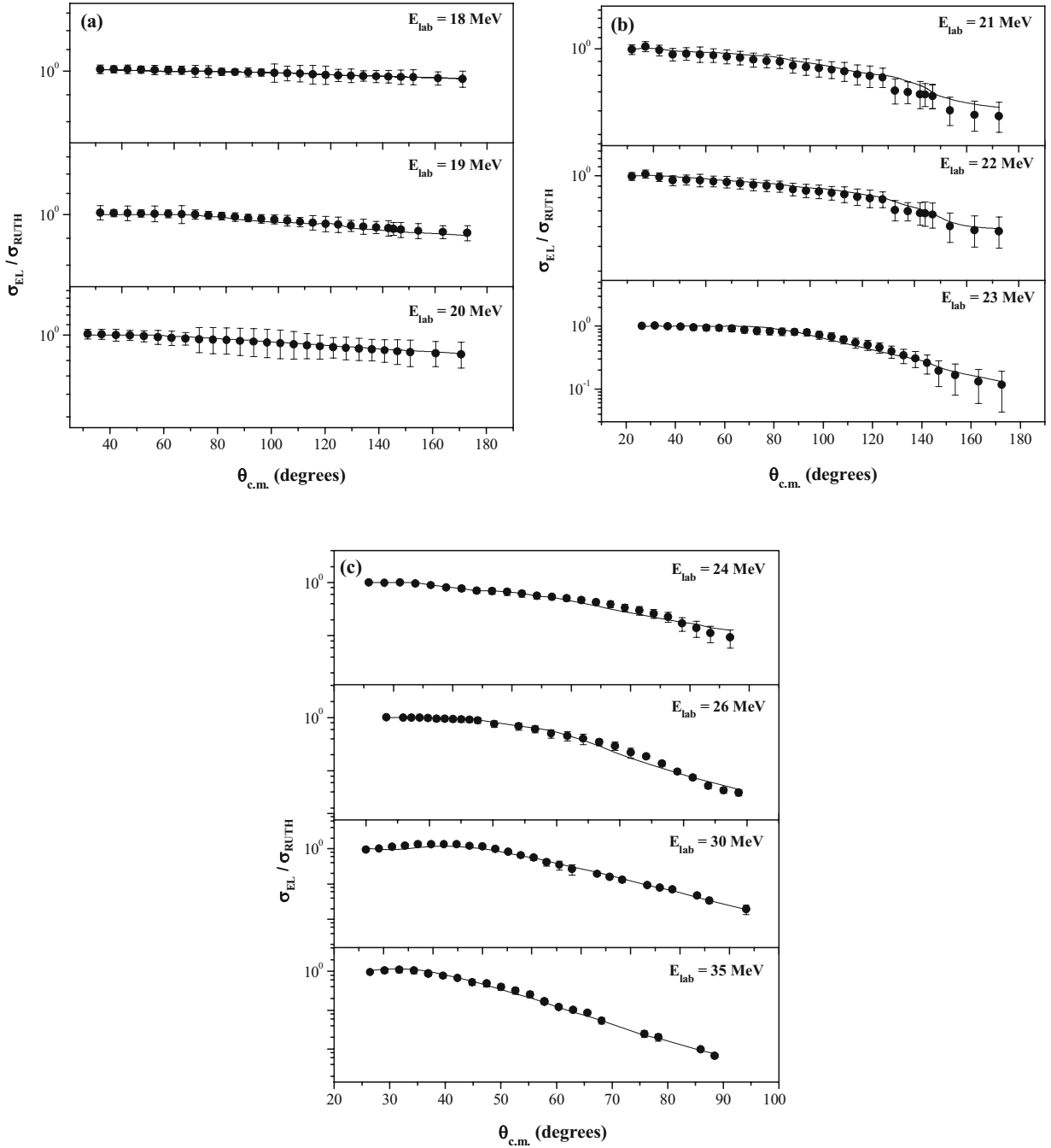
Fig. 2. (a) Experimental elastic-scattering cross-sections normalized to the Rutherford cross-sections for the ^{7}Li $+$ ^{116}Sn system at energies $E_{\mathrm{lab}} = 18$–20 MeV and their best fits from optical-model calculations. The curves correspond to the best fits obtained using the Woods-Saxon potential (WSP); (b) same as (a) but for energies $E_{\mathrm{lab}} = 21$–23 MeV; (c) same as (a) but for energies $E_{\mathrm{lab}} = 24$–35 MeV.

the imaginary potential is also not observed. The explanation for that should be that the attractive polarization potential due to the ^{7}Li bound excited state and transfer channels is of similar strength as the repulsive polarization potential due to the breakup for these systems. Also, very recently it has been shown [26,27] that an important fraction of the ^{7}Li breakup is not a direct mechanism, but rather a sequential process where the stripping of one neutron and the pickup of one proton take place before the breakup. These first step transfer reactions may decrease the strength of the repulsive breakup polarization potential, as compared with pure direct breakup of ^{7}Li. On the other hand, if one compares the present results with those from our previous measurements of elastic-scattering data for the ^{6}Li $+$ ^{116}Sn system [9], one finds that the later has a behaviour more compatible with the BTA, since there is

Table 1. Parameters used with Woods-Saxon potential calculations for the ^{7}Li + ^{116}Sn system and the derived total reaction cross-sections.

E_{lab} (MeV)	V_r (MeV)	V_i (MeV)	R_v and R_i (fm)	a_r and a_i (fm)	χ^2/n	σ_R (mb)
18	2500	3850	7.20	0.45	0.30	21
19	2550	3450	7.20	0.45	2.32	55
20	2580	3500	7.20	0.45	0.88	128
21	757	901	7.20	0.53	3.10	257
22	550	616	7.20	0.53	1.33	327
23	349	552	7.20	0.53	0.67	405
24	855	600	7.20	0.53	4.00	635
26	498	255	7.20	0.53	1.71	730
30	565	61	7.20	0.53	0.81	1059
35	789	31.5	7.20	0.53	6.83	1444
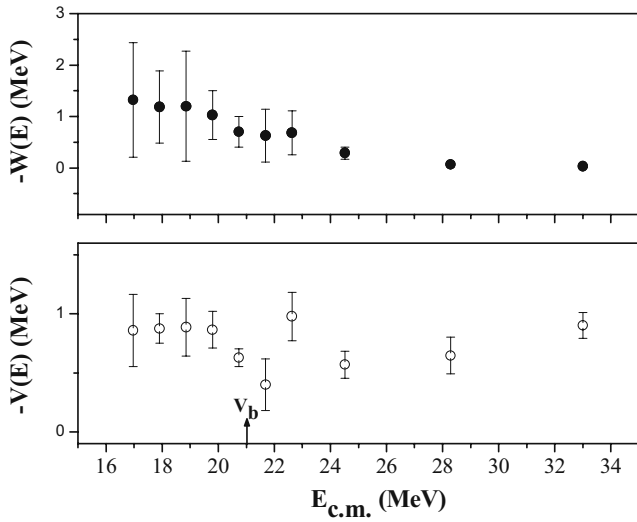
Fig. 3. Energy dependence of the real and imaginary parts of the optical potential obtained for the ^{7}Li + ^{116}Sn system at an average radius $R_S = 9.685$ fm. The energy V_b of the Coulomb barrier is shown by the arrow.

a trend of increasing the imaginary potential at energies below the barrier and some corresponding decrease of the real potential, as the bombarding energy decreases. The reason for these different behaviours between the two Li isotopes should be mainly due to the absence of bound excited state in ^{6}Li and lower threshold energy for breakup than for ^{7}Li. Also, most of the ^{6}Li breakup seems to be direct breakup [26,28] rather than breakup following transfer.

4 Total reaction cross-sections

The total reaction cross-sections obtained for the ^{7}Li + ^{116}Sn system, which is derived from the optical model fitting of the experimental data is shown in the last column of table 1. In our previous work [9] on the

scattering of ^{6}Li on ^{112,116}Sn, we have compared the derived total reaction cross-sections for those systems with some other weakly and tightly bound systems. In the present paper we compare the total reaction cross-sections between the ^{6}Li + ^{116}Sn and ^{7}Li + ^{116}Sn systems. Figures 4(a) and (b) show the comparison by the two reduction methods widely used to compare cross-sections of different systems in the same plot. Figure 4(a) uses the method proposed by Gomes *et al.* [29] and fig. 4(b) uses the method proposed by Canto *et al.* [30,31] for fusion cross-sections and later extended by Shorto *et al.* [32] for total reaction cross-sections. A brief description of both methods can be found in ref. [9]. One can observe that by both methods the total reaction cross-section for the ^{6}Li + ^{116}Sn system is larger than for the ^{7}Li + ^{116}Sn system. So, the different behaviour of the energy dependence of the optical potential for these two systems is reflected in the total reaction cross-section values. In the ^{6}Li scattering, the breakup plays a more important role than in the ^{7}Li scattering. The breakup cross-section for ^{6}Li should be larger than for ^{7}Li, and consequently, the total reaction cross-section is larger for reactions induced by ^{6}Li than by ^{7}Li.

5 Conclusions

In order to contribute to the investigation of the presence of the threshold anomaly or breakup threshold anomaly in the optical potential of the scattering of weakly bound systems, elastic-scattering angular distributions have been measured for the ^{7}Li + ^{116}Sn system at energies around and below the Coulomb barrier. The present analysis suggests the absence of the threshold anomaly due to the almost energy independence of the real and imaginary parts of the optical potential. This result is in agreement with those obtained for the scattering of ^{7}Li by heavier and lighter targets. On the other hand, several systems with ^{6}Li as projectile show a clear behaviour typical of the breakup threshold anomaly, including the one with the same ^{116}Sn target. We explain these behaviours by
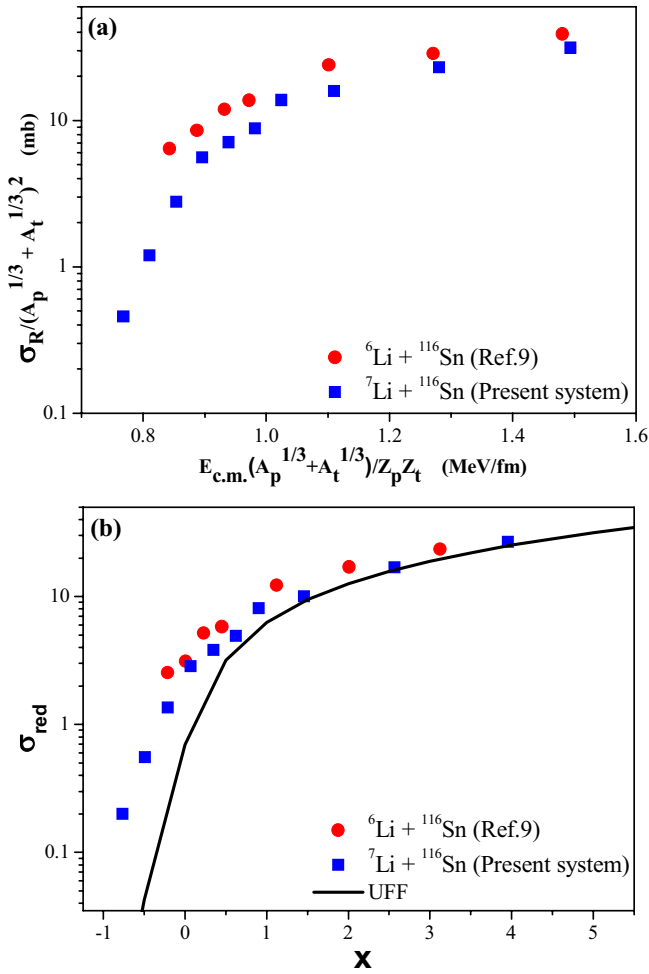
Fig. 4. (Color online) Total reaction cross-sections for the ^{6,7}Li $+$ ^{116}Sn systems. On the upper panel, (a), the reduction method is proposed in ref. [29] and on the lower panel, (b), the reduction method is proposed in refs. [30–32].

the fact that the scattering of weakly bound nuclei are affected by the repulsive polarization potential produced by the breakup process, important even at energies below the Coulomb barrier, but, for the specific case of ^{7}Li, there is a strong competition between this repulsive polarization potential and the attractive polarization potential produced by the bound ^{7}Li excited state and transfer reactions. For ^{7}Li, these two components of the polarization potential have similar strengths and the net result is an almost energy-independent optical potential. This result cannot be extrapolated for every target, because the relative importance of the polarization potential produced by the different reaction mechanisms may vary with the target structure. The total reaction cross-section for the ^{6}Li $+$ ^{116}Sn system is larger than for ^{7}Li $+$ ^{116}Sn system, corresponding to larger breakup cross-section for the former than for the later.

References

1. M.A. Nagarajan, C.C. Mahaux, G.R. Satchler, Phys. Rev. Lett. **54**, 1136 (1985).
2. G.R. Satchler, Phys. Rep. **199**, 147 (1991).
3. M.E. Brandan, G.R. Satchler, Phys. Rep. **285**, 143 (1997).
4. P.R.S. Gomes *et al.*, J. Phys. G **31**, S1669 (2005).
5. M.S. Hussein *et al.*, Phys. Rev. C **73**, 044610 (2006).
6. M.S. Hussein, P.R.S. Gomes, J. Lubian, L.C. Chamon, private communication.
7. K. Zerva *et al.*, Phys. Rev. C **80**, 017601 (2009).
8. K. Zerva *et al.*, Phys. Rev. C **82**, 044607 (2010).
9. N.N. Deshmukh *et al.*, Phys. Rev. C **83**, 024607 (2011).
10. J.M. Figueira *et al.*, Phys. Rev. C **75**, 017602 (2007).
11. A. Gomez Camacho *et al.*, Nucl. Phys. A **833**, 156 (2010).
12. M. Biswas *et al.*, Nucl. Phys. A **802**, 67 (2008).
13. M. Zadro *et al.*, Phys. Rev. C **80**, 064610 (2009).
14. H. Kumawat *et al.*, Phys. Rev. C **78**, 044617 (2008).
15. J.M. Figueira *et al.*, Phys. Rev. C **81**, 024603 (2010).
16. N. Keeley *et al.*, Nucl. Phys. A **571**, 326 (1994).
17. S. Santra *et al.*, Phys. Rev. C **83**, 034616 (2011).
18. J. Lubian *et al.*, Nucl. Phys. A **791**, 24 (2007).
19. A. Pakou *et al.*, Phys. Lett. B **556**, 21 (2003).
20. A. Pakou *et al.*, Phys. Rev. C **69**, 054602 (2004).
21. J.M. Figueira *et al.*, Phys. Rev. C **73**, 054603 (2006).
22. F.A. Souza *et al.*, Phys. Rev. C **75**, 044601 (2007).
23. J. Lubian *et al.*, Phys. Rev. C **64**, 027601 (2001).
24. A.M.M. Maciel *et al.*, Phys. Rev. C **59**, 2103 (1999).
25. J. Raynal, Phys. Rev. C **23**, 2571 (1981).
26. D.H. Luang *et al.*, Phys. Lett. B **695**, 105 (2011).
27. D. Martinez Heimann *et al.*, Nucl. Instrum. Methods Phys. Res. A **622**, 642 (2010).
28. O.A. Capurro *et al.*, Nucl. Phys. A **849**, 1 (2011).
29. P.R.S. Gomes *et al.*, Phys. Rev. C **71**, 017601 (2005).
30. L.F. Canto *et al.*, J. Phys. G **36**, 015109 (2009).
31. L.F. Canto *et al.*, Nucl. Phys. A **821**, 51 (2009).
32. J.M.B. Shorto *et al.*, Phys. Lett. B **678**, 77 (2009).